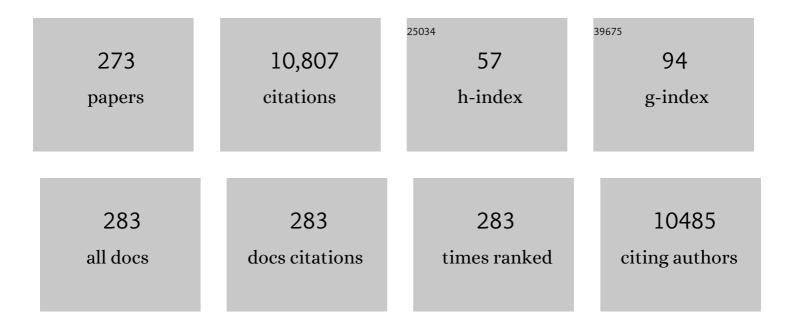
Tadaaki Nagao

List of Publications by Year in descending order

Source: https://exaly.com/author-pdf/5624238/publications.pdf

Version: 2024-02-01



ΤΑΠΑΛΚΙ ΝΑCAO

#	Article	IF	CITATIONS
1	Direct imaging of visible-light-induced one-step charge separation at the chromium(<scp>iii</scp>) oxide–strontium titanate interface. Journal of Materials Chemistry A, 2022, 10, 752-761.	10.3	6
2	Solar Water Distillation Using Titanium Nitride Nanostructures. Journal of the Society of Powder Technology, Japan, 2022, 59, 79-82.	0.1	0
3	Photothermal heating and heat transfer analysis of anodic aluminum oxide with high optical absorptance. Nanophotonics, 2022, 11, 3375-3381.	6.0	4
4	A temperature programmed desorption study of interactions between water and hydrophobes at cryogenic temperatures. Physical Chemistry Chemical Physics, 2022, 24, 16900-16907.	2.8	1
5	Extreme thermal anisotropy in high-aspect-ratio titanium nitride nanostructures for efficient photothermal heating. Nanophotonics, 2021, 10, 1487-1494.	6.0	18
6	Quantifying photoinduced carriers transport in exciton–polariton coupling of MoS2 monolayers. Npj 2D Materials and Applications, 2021, 5, .	7.9	12
7	Hydropower generation by transpiration from microporous alumina. Scientific Reports, 2021, 11, 10954.	3.3	15
8	Simultaneous harvesting of radiative cooling and solar heating for transverse thermoelectric generation. Science and Technology of Advanced Materials, 2021, 22, 441-448.	6.1	9
9	Uniaxially oriented nickel aluminum superalloy films sputtered with in situ heating. Applied Physics Express, 2021, 14, 087001.	2.4	0
10	Triggering Water and Methanol Activation for Solar-Driven H ₂ Production: Interplay of Dual Active Sites over Plasmonic ZnCu Alloy. Journal of the American Chemical Society, 2021, 143, 12145-12153.	13.7	85
11	Carbon Dot/Cellulose-Based Transparent Films for Efficient UV and High-Energy Blue Light Screening. ACS Sustainable Chemistry and Engineering, 2021, 9, 9879-9890.	6.7	28
12	Transparent Hard Coatings with SiON-Encapsulated N-Doped Carbon Dots for Complete UV Blocking and White Light Emission. ACS Applied Electronic Materials, 2021, 3, 3761-3773.	4.3	13
13	Plasmon-induced Charge Transport at Transition Metal Nitride-Semiconductor Interfaces via In Situ Nanoimaging. , 2021, , .		0
14	Solar-active titanium-based oxide photocatalysts loaded on TiN array absorbers for enhanced broadband photocurrent generation. Journal of Applied Physics, 2021, 129, .	2.5	6
15	Effects of Ag particle geometry on photocatalytic performance of Ag/TiO2/reduced graphene oxide ternary systems. Materials Chemistry and Physics, 2020, 240, 122216.	4.0	16
16	Nanoantenna Structure with Mid-Infrared Plasmonic Niobium-Doped Titanium Oxide. Micromachines, 2020, 11, 23.	2.9	5
17	Direct Observation of Photoinduced Charge Separation at Transition-Metal Nitride–Semiconductor Interfaces. ACS Applied Materials & Interfaces, 2020, 12, 56562-56567.	8.0	10
18	Device Architecture for Visible and Near-Infrared Photodetectors Based on Two-Dimensional SnSe2 and MoS2: A Review. Micromachines, 2020, 11, 750.	2.9	19

#	ŧ	Article	IF	CITATIONS
1	.9	Editorial for the Special Issue "Infrared Nanophotonics: Materials, Devices and Applicationsâ€. Micromachines, 2020, 11, 808.	2.9	0
2	20	Optical microresonator arrays of fluorescence-switchable diarylethenes with unreplicable spectral fingerprints. Materials Horizons, 2020, 7, 1801-1808.	12.2	36
2	21	Graphene-Loaded Plasmonic Zirconium Nitride and Gold Nanogroove Arrays for Surface-Charge Modifications. ACS Applied Nano Materials, 2020, 3, 5002-5007.	5.0	8
2	22	Marimo-Bead-Supported Core–Shell Nanocomposites of Titanium Nitride and Chromium-Doped Titanium Dioxide as a Highly Efficient Water-Floatable Green Photocatalyst. ACS Applied Materials & Interfaces, 2020, 12, 31327-31339.	8.0	24
2	23	Ultrafast optical modulation of Dirac electrons in gated single-layer graphene. Physical Review B, 2020, 101, .	3.2	7
2	24	Optical phase change in bismuth through structural distortions induced by laser irradiation. Radiation Effects and Defects in Solids, 2020, 175, 291-306.	1.2	1
2	25	Enhanced photocurrent generation from indium–tin-oxide/Fe2TiO5 hybrid nanocone arrays. Nano Energy, 2020, 76, 104965.	16.0	9
2	26	Radiative cooling for continuous thermoelectric power generation in day and night. Applied Physics Letters, 2020, 117, .	3.3	62
2	27	Narrowâ€Band Thermal Emitter with Titanium Nitride Thin Film Demonstrating High Temperature Stability. Advanced Optical Materials, 2020, 8, 1900982.	7.3	34
2	28	Dual roles of a transparent polymer film containing dispersed N-doped carbon dots: A high-efficiency blue light converter and UV screen. Applied Surface Science, 2020, 510, 145405.	6.1	36
2	29	Epitaxial growth mechanism of high-crystallinity lanthanum hexaboride (001) thin films on silicon (001) by electron beam deposition. Applied Physics Express, 2020, 13, 055504. Combined first-principles and electromagnetic simulation study of <mml:math< td=""><td>2.4</td><td>4</td></mml:math<>	2.4	4
3	80	xmlns:mml="http://www.w3.org/1998/Math/MathML"> <mml:mi>n</mml:mi> -type doped anatase <mml:math xmlns:mml="http://www.w3.org/1998/Math/MathML"><mml:mi>n</mml:mi>Ti<mml:msub><mml:mi mathvariant="normal">O<mml:mn>2</mml:mn></mml:mi </mml:msub> for</mml:math 	2.4	2
3	31	the applications in infrared surface plasmon photonics. Physical Review Materials, 2020, 4, . Photocomposites with Gold Nanostructures/Reduced Graphene Oxide on Nanobranched Substrate. Journal of Physical Chemistry C, 2019, 123, 21103-21113.	3.1	33
3	32	Unconventional energy transfer from narrow to broad luminescent wide band gap materials. Europhysics Letters, 2019, 127, 17003.	2.0	1
3	3	High quality thermochromic VO2 films prepared by magnetron sputtering using V2O5 target with in situ annealing. Applied Surface Science, 2019, 495, 143436.	6.1	44
3	34	Dark-Field Scattering and Local SERS Mapping from Plasmonic Aluminum Bowtie Antenna Array. Micromachines, 2019, 10, 468.	2.9	8
3	5	A MEMS-Based Quad-Wavelength Hybrid Plasmonic–Pyroelectric Infrared Detector. Micromachines, 2019, 10, 413.	2.9	16
3	6	MEMS-Based Wavelength-Selective Bolometers. Micromachines, 2019, 10, 416.	2.9	19

#	Article	IF	CITATIONS
37	An Onâ€Chip Quadâ€Wavelength Pyroelectric Sensor for Spectroscopic Infrared Sensing. Advanced Science, 2019, 6, 1900579.	11.2	31
38	Ultrafast carrier generation in Bi1-xSbx thin films induced by intense monocycle terahertz pulses. EPJ Web of Conferences, 2019, 205, 04016.	0.3	0
39	Thermochromic vanadium dioxide film on textured silica substrate for smart window with enhanced visible transmittance and tunable infrared radiation. Infrared Physics and Technology, 2019, 102, 103019.	2.9	10
40	Optical Properties of Au-Based and Pt-Based Alloys for Infrared Device Applications: A Combined First Principle and Electromagnetic Simulation Study. Micromachines, 2019, 10, 73.	2.9	7
41	Ultranarrow-Band Wavelength-Selective Thermal Emission with Aperiodic Multilayered Metamaterials Designed by Bayesian Optimization. ACS Central Science, 2019, 5, 319-326.	11.3	121
42	Structure and optical properties of sputter deposited pseudobrookite Fe ₂ TiO ₅ thin films. CrystEngComm, 2019, 21, 34-40.	2.6	30
43	Optoelectronic characteristics of the Ag-doped Si p-n photodiodes prepared by a facile thermal diffusion process. AIP Advances, 2019, 9, 055024.	1.3	4
44	Laser-induced structural disordering and optical phase change in semimetal bismuth observed by Raman microscopy. Applied Surface Science, 2019, 491, 675-681.	6.1	13
45	Sub-Band Gap Photodetection from the Titanium Nitride/Germanium Heterostructure. ACS Applied Materials & Interfaces, 2019, 11, 21965-21972.	8.0	28
46	Dual-band <i>in situ</i> molecular spectroscopy using single-sized Al-disk perfect absorbers. Nanoscale, 2019, 11, 9508-9517.	5.6	22
47	Photo-assisted methanol synthesis via CO2 reduction under ambient pressure over plasmonic Cu/ZnO catalysts. Applied Catalysis B: Environmental, 2019, 250, 10-16.	20.2	142
48	Terahertz Faraday and Kerr rotation spectroscopy of <mml:math xmlns:mml="http://www.w3.org/1998/Math/MathML"><mml:mrow><mml:msub><mml:mi>Bi</mml:mi><mml:m films in high magnetic fields up to 30 tesla. Physical Review B, 2019, 100, .</mml:m </mml:msub></mml:mrow></mml:math 	ro &.2 <mr< td=""><td>าl:mธ>1</td></mr<>	า l:mธ >1
49	Allâ€Ceramic Solarâ€Driven Water Purifier Based on Anodized Aluminum Oxide and Plasmonic Titanium Nitride. Advanced Sustainable Systems, 2019, 3, 1800112.	5.3	67
50	Nonmetallic Materials for Plasmonic Hot Carrier Excitation. Advanced Optical Materials, 2019, 7, 1800603.	7.3	58
51	Gires-Tournois resonators as ultra-narrowband perfect absorbers for infrared spectroscopic devices. Optics Express, 2019, 27, A725.	3.4	8
52	Selective thermal emitters with infrared plasmonic indium tin oxide working in the atmosphere. Optical Materials Express, 2019, 9, 2534.	3.0	20
53	Optical Excitation of Hot Carriers and Photothermal Conversions with Transition Metal Nitrides and Transition Metal Carbides. The Review of Laser Engineering, 2019, 47, 365.	0.0	0
54	Light-promoted conversion of greenhouse gases over plasmonic metal–carbide nanocomposite catalysts. Materials Chemistry Frontiers, 2018, 2, 580-584.	5.9	20

Ταδαακί Νάδαο

#	Article	IF	CITATIONS
55	Enhanced Solar Light Absorption and Photoelectrochemical Conversion Using TiN Nanoparticle-Incorporated C ₃ N ₄ –C Dot Sheets. ACS Applied Materials & Interfaces, 2018, 10, 2460-2468.	8.0	64
56	Fabrication of Highly Metallic TiN Films by Pulsed Laser Deposition Method for Plasmonic Applications. ACS Photonics, 2018, 5, 814-819.	6.6	60
57	Light-Enhanced Carbon Dioxide Activation and Conversion by Effective Plasmonic Coupling Effect of Pt and Au Nanoparticles. ACS Applied Materials & Interfaces, 2018, 10, 408-416.	8.0	179
58	FRET-mediated near infrared whispering gallery modes: studies on the relevance of intracavity energy transfer with <i>Q</i> -factors. Materials Chemistry Frontiers, 2018, 2, 270-274.	5.9	26
59	Photocurrent Generation with Transition Metal Nitrides and Transition Metal Carbides. , 2018, , .		1
60	Harvesting Sunlight with Titanium Nitride Nanostructures. , 2018, , .		2
61	Role of Gap Size and Gap Density of the Plasmonic Random Gold Nanoisland Ensemble for Surface-Enhanced Raman Spectroscopy. Materials Transactions, 2018, 59, 1081-1086.	1.2	3
62	Demonstration of temperature-plateau superheated liquid by photothermal conversion of plasmonic titanium nitride nanostructures. Nanoscale, 2018, 10, 18451-18456.	5.6	24
63	Effect of oxygen annealing on the photoresponse of PbSe thin films fabricated by the pulsed laser deposition method. Radiation Effects and Defects in Solids, 2018, 173, 112-117.	1.2	13
64	Metal/Conductive Oxide Plasmonic Structures for Surface-Enhanced Infrared Absorption Spectroscopy. Bunseki Kagaku, 2018, 67, 81-94.	0.2	1
65	A synergistic interaction between isolated Au nanoparticles and oxygen vacancies in an amorphous black TiO ₂ nanoporous film: toward enhanced photoelectrochemical water splitting. Journal of Materials Chemistry A, 2018, 6, 12978-12984.	10.3	44
66	Broadband Plasmon Resonance Enhanced Third-Order Optical Nonlinearity in Refractory Titanium Nitride Nanostructures. ACS Photonics, 2018, 5, 3452-3458.	6.6	33
67	Ultra-Narrowband Wavelength-Selective Thermal Emitter Designed by Bayesian Optimization. The Proceedings of the Thermal Engineering Conference, 2018, 2018, 0135.	0.0	0
68	Nonlinear terahertz dynamics of Dirac electrons in Bi thin films. , 2018, , .		0
69	Enhanced photoelectrochemical water splitting by plasmonic Au nanostructures/reduced graphene oxide. , 2018, , .		0
70	Plasmonic–Photonic Hybrid Modes Excited on a Titanium Nitride Nanoparticle Array in the Visible Region. ACS Photonics, 2017, 4, 815-822.	6.6	26
71	Resonant Optical Absorption and Photothermal Process in High Refractive Index Germanium Nanoparticles. Advanced Optical Materials, 2017, 5, 1600902.	7.3	34
72	UV-visible light photocurrent enhancement in STO thin films through metal-defect co-doping effect combined with Au plasmons. Materials Express, 2017, 7, 66-71.	0.5	1

Ταδαακί Νάδαο

#	Article	lF	CITATIONS
73	Midâ€infrared optical and electrical properties of indium tin oxide films. Physica Status Solidi (A) Applications and Materials Science, 2017, 214, 1600467.	1.8	18
74	Light assisted CO ₂ reduction with methane over SiO ₂ encapsulated Ni nanocatalysts for boosted activity and stability. Journal of Materials Chemistry A, 2017, 5, 10567-10573.	10.3	71
75	Proteinâ€Functionalized Indiumâ€Tin Oxide Nanoantenna Arrays for Selective Infrared Biosensing. Advanced Optical Materials, 2017, 5, 1700091.	7.3	23
76	White Light Emission from Black Germanium. ACS Photonics, 2017, 4, 1722-1729.	6.6	11
77	Tunable Nanoantennas for Surface Enhanced Infrared Absorption Spectroscopy by Colloidal Lithography and Post-Fabrication Etching. Scientific Reports, 2017, 7, 44069.	3.3	37
78	Light assisted CO 2 reduction with methane over group VIII metals: Universality of metal localized surface plasmon resonance in reactant activation. Applied Catalysis B: Environmental, 2017, 209, 183-189.	20.2	122
79	Far-field and near-field monitoring of hybridized optical modes from Au nanoprisms suspended on a graphene/Si nanopillar array. Nanoscale, 2017, 9, 16950-16959.	5.6	10
80	Wavelength-selective spin-current generator using infrared plasmonic metamaterials. APL Photonics, 2017, 2, .	5.7	12
81	Sub-10 nm, high density titania nanoforests–gold nanoparticles composite for efficient sunlight-driven photocatalysis. Japanese Journal of Applied Physics, 2017, 56, 095001.	1.5	3
82	All-Ceramic Microfibrous Solar Steam Generator: TiN Plasmonic Nanoparticle-Loaded Transparent Microfibers. ACS Sustainable Chemistry and Engineering, 2017, 5, 8523-8528.	6.7	93
83	Narrowband Wavelength Selective Thermal Emitters by Confined Tamm Plasmon Polaritons. ACS Photonics, 2017, 4, 2212-2219.	6.6	164
84	Improvement of smooth surface of RuO2 bottom electrode on Al2O3 buffer layer and characteristics of RuO2/TiO2/Al2O3/TiO2/RuO2 capacitors. Journal of Vacuum Science and Technology A: Vacuum, Surfaces and Films, 2017, 35, .	2.1	8
85	Photocurrent generation from TiN nanostructures by visible light. , 2017, , .		1
86	Strong coupling between phonon-polaritons and plasmonic nanorods. Optics Express, 2016, 24, 25528.	3.4	39
87	Tamm plasmon selective thermal emitters. Optics Letters, 2016, 41, 4453.	3.3	58
88	Effects of nanoscale morphology and defects in oxide: optoelectronic functions of zinc oxide nanowires. Radiation Effects and Defects in Solids, 2016, 171, 22-33.	1.2	9
89	Plasmon-mediated photothermal conversion by TiN nanocubes toward CO oxidation under solar light illumination. RSC Advances, 2016, 6, 110566-110570.	3.6	17
90	Conjugated Polymer Blend Microspheres for Efficient, Long-Range Light Energy Transfer. ACS Nano, 2016, 10, 5543-5549.	14.6	46

#	Article	IF	CITATIONS
91	Hot Electron Excitation from Titanium Nitride Using Visible Light. ACS Photonics, 2016, 3, 1552-1557.	6.6	98
92	Aluminum infrared plasmonic perfect absorbers for wavelength selective devices. Proceedings of SPIE, 2016, , .	0.8	1
93	Plasmonic mesostructures with aligned hotspots on highly oriented mesoporous silica films. Optical Materials Express, 2016, 6, 2824.	3.0	5
94	Spectrally Selective Midâ€Infrared Thermal Emission from Molybdenum Plasmonic Metamaterial Operated up to 1000 °C. Advanced Optical Materials, 2016, 4, 1987-1992.	7.3	79
95	Metamaterial-enhanced vibrational absorption spectroscopy for the detection of protein molecules. Scientific Reports, 2016, 6, 32123.	3.3	63
96	Ensemble of gold-patchy nanoparticles with multiple hot-spots for plasmon-enhanced vibrational spectroscopy. Proceedings of SPIE, 2016, , .	0.8	2
97	Surfaceâ€Plasmonâ€Enhanced Photodriven CO ₂ Reduction Catalyzed by Metal–Organicâ€Frameworkâ€Derived Iron Nanoparticles Encapsulated by Ultrathin Carbon Layers. Advanced Materials, 2016, 28, 3703-3710.	21.0	300
98	Hole Array Perfect Absorbers for Spectrally Selective Midwavelength Infrared Pyroelectric Detectors. ACS Photonics, 2016, 3, 1271-1278.	6.6	92
99	Synthesis, structural, and electrical characterization of RuO2 sol–gel spin-coating nano-films. Journal of Materials Science: Materials in Electronics, 2016, 27, 10791-10797.	2.2	14
100	Design of PdAu alloy plasmonic nanoparticles for improved catalytic performance in CO2 reduction with visible light irradiation. Nano Energy, 2016, 26, 398-404.	16.0	133
101	Self-assembled polycarbazole microspheres as single-component, white-colour resonant photoemitters. RSC Advances, 2016, 6, 52854-52857.	3.6	13
102	Color-Tunable Resonant Photoluminescence and Cavity-Mediated Multistep Energy Transfer Cascade. ACS Nano, 2016, 10, 7058-7063.	14.6	67
103	Examining the Performance of Refractory Conductive Ceramics as Plasmonic Materials: A Theoretical Approach. ACS Photonics, 2016, 3, 43-50.	6.6	126
104	Band engineering of ternary metal nitride system Ti_1-x Zr_xN for plasmonic applications. Optical Materials Express, 2016, 6, 29.	3.0	37
105	Solar water heating and vaporization with silicon nanoparticles at mie resonances. Optical Materials Express, 2016, 6, 640.	3.0	69
106	Hybridizing Poly(Îμ-caprolactone) and Plasmonic Titanium Nitride Nanoparticles for Broadband Photoresponsive Shape Memory Films. ACS Applied Materials & Interfaces, 2016, 8, 5634-5640.	8.0	59
107	Titanium Nitride Nanoparticles as Plasmonic Solar Heat Transducers. Journal of Physical Chemistry C, 2016, 120, 2343-2348.	3.1	273

108 Fabrication and Characterization of Moiré Metasurfaces. , 2016, , .

0

#	Article	IF	CITATIONS
109	Enhanced photocatalytic activity of ultra-high aspect ratio ZnO nanowires due to Cu induced defects. Radiation Effects and Defects in Solids, 2015, 170, 939-944.	1.2	1
110	Ultrafast phonon dynamics of epitaxial atomic layers of Bi on Si(111). Physical Review B, 2015, 91, .	3.2	19
111	Plasmon mediated cathodic photocurrent generation in sol-gel synthesized doped SrTiO3 nanofilms. APL Materials, 2015, 3, .	5.1	6
112	Electron Dynamics in a Gold Thin Film Accelerated via an Intense Terahertz Field. , 2015, , .		0
113	Terahertz-induced acceleration of massive Dirac electrons in semimetal bismuth. Scientific Reports, 2015, 5, 15870.	3.3	13
114	Conversion of Carbon Dioxide by Methane Reforming under Visible‣ight Irradiation: Surfaceâ€Plasmonâ€Mediated Nonpolar Molecule Activation. Angewandte Chemie - International Edition, 2015, 54, 11545-11549.	13.8	168
115	Infrared Aluminum Metamaterial Perfect Absorbers for Plasmonâ€Enhanced Infrared Spectroscopy. Advanced Functional Materials, 2015, 25, 6637-6643.	14.9	129
116	Excitation Induced Tunable Emission in Ce ^{3+} /Eu ^{3+} Codoped BiPO _{4} Nanophosphors. Journal of Spectroscopy, 2015, 2015, 1-10.	1.3	14
117	Infrared Perfect Absorbers Fabricated by Colloidal Mask Etching of Al–Al ₂ 0 ₃ –Al Trilayers. ACS Photonics, 2015, 2, 964-970.	6.6	172
118	Moiré Nanosphere Lithography. ACS Nano, 2015, 9, 6031-6040.	14.6	91
119	Lossy plasmonic resonances in nanoparticles for broadband light absorption. , 2015, , .		0
120	Moir $ ilde{A}$ © nanosphere lithography: use colloidal moir $ ilde{A}$ © patterns as masks. Proceedings of SPIE, 2015, , .	0.8	1
121	Plasmon-mediated photocatalytic activity of wet-chemically prepared ZnO nanowire arrays. Physical Chemistry Chemical Physics, 2015, 17, 7395-7403.	2.8	29
122	Terahertz-Field-Induced Nonlinear Electron Delocalization in Au Nanostructures. Nano Letters, 2015, 15, 1036-1040.	9.1	34
123	Whispering Gallery Resonance from Self-Assembled Microspheres of Highly Fluorescent Isolated Conjugated Polymers. Macromolecules, 2015, 48, 3928-3933.	4.8	45
124	Fabrication of plasmonic nanopillar arrays based on nanoforming. Microelectronic Engineering, 2015, 139, 7-12.	2.4	8
125	Insulator-to-Proton-Conductor Transition in a Dense Metal–Organic Framework. Journal of the American Chemical Society, 2015, 137, 6428-6431.	13.7	83
126	Electrochemical synthesis of mesoporous gold films toward mesospace-stimulated optical properties. Nature Communications, 2015, 6, 6608.	12.8	178

Ταdaaki Nagao

#	Article	IF	CITATIONS
127	Transparent oxides forming conductor/insulator/conductor heterojunctions for photodetection. Nanotechnology, 2015, 26, 215203.	2.6	8
128	Anti-reflection textured structures by wet etching and island lithography for surface-enhanced Raman spectroscopy. Applied Surface Science, 2015, 357, 615-621.	6.1	20
129	Sunlight absorbing titanium nitride nanoparticles. , 2015, , .		4
130	Tunable multiband metasurfaces by moir $ ilde{A}$ © nanosphere lithography. Nanoscale, 2015, 7, 20391-20396.	5.6	29
131	Selective patterned growth of ZnO nanowires/nanosheets and their photoluminescence properties. Optical Materials Express, 2015, 5, 353.	3.0	21
132	Active molecular plasmonics: tuning surface plasmon resonances by exploiting molecular dimensions. Nanophotonics, 2015, 4, 186-197.	6.0	26
133	Effect of different surfactants on structural and optical properties of Ce3+ and Tb3+ co-doped BiPO4 nanostructures. Optical Materials, 2015, 39, 110-117.	3.6	34
134	Nonlinear Carrier Dynamics in Semi-metal Bismuth Induced by Intense Terahertz Field. Springer Proceedings in Physics, 2015, , 633-636.	0.2	0
135	Nonlinear electron dynamics of gold ultrathin films induced by intense terahertz waves. Applied Physics Letters, 2014, 105, .	3.3	4
136	Carrier Dynamics of a Bismuth Thin Film Accelerated via Intense Terahertz Field. , 2014, , .		0
137	Nonlinear Carrier Responses in Gold Thin Films Induced by Intense Terahertz Waves. , 2014, , .		0
138	Nonlinear Carrier Dynamics in Semi-Metal Bismuth Induced by Intense Terahertz Field. , 2014, , .		0
139	Electron- and photon-induced plasmonic excitations in two-dimensional silver nanostructures. Applied Physics Letters, 2014, 104, 251117.	3.3	3
140	Optical properties of ordered Dot-on-Plate nano-sandwich arrays. Microelectronic Engineering, 2014, 127, 34-39.	2.4	6
141	Effective decoration of Pd nanoparticles on the surface of SnO2 nanowires for enhancement of CO gas-sensing performance. Journal of Hazardous Materials, 2014, 265, 124-132.	12.4	125
142	Visible-light photodecomposition of acetaldehyde by TiO ₂ -coated gold nanocages: plasmon-mediated hot electron transport via defect states. Chemical Communications, 2014, 50, 15553-15556.	4.1	33
143	Plasmonic Janus omposite Photocatalyst Comprising Au and C–TiO ₂ for Enhanced Aerobic Oxidation over a Broad Visibleâ€Light Range. Advanced Functional Materials, 2014, 24, 7754-7762.	14.9	83
144	Design of a silicon-based plasmonic optical sensor for magnetic field monitoring in the infrared. Applied Physics B: Lasers and Optics, 2014, 117, 363-368.	2.2	13

Ταdaaki Nagao

#	Article	IF	CITATIONS
145	Magnetically Assembled Ni@Ag Urchinâ€Like Ensembles with Ultraâ€Sharp Tips and Numerous Caps for SERS Applications. Small, 2014, 10, 2564-2569.	10.0	18
146	Monitoring the Presence of Ionic Mercury in Environmental Water by Plasmon-Enhanced Infrared Spectroscopy. Scientific Reports, 2013, 3, 1175.	3.3	98
147	Arrays of Nanoscale Gold Dishes Containing Engineered Substructures. Advanced Optical Materials, 2013, 1, 814-818.	7.3	8
148	Chemically synthesized nanowire TiO2/ZnO core-shell p-n junction array for high sensitivity ultraviolet photodetector. Applied Physics Letters, 2013, 103, .	3.3	52
149	Edge States of Bi Nanoribbons on Bi Substrates: First-Principles Density Functional Study. Japanese Journal of Applied Physics, 2012, 51, 025201.	1.5	6
150	Fabrication of Highly Dense Nanoholes by Self-Assembled Gallium Droplet on Silicon Surface. Materials Express, 2012, 2, 245-250.	0.5	3
151	Carbon nanotube mat as substrate for ZnO nanotip field emitters. RSC Advances, 2012, 2, 2713.	3.6	10
152	Porous gold nanodisks with multiple internal hot spots. Physical Chemistry Chemical Physics, 2012, 14, 9131.	2.8	48
153	Angstrom-Scale Distance Dependence of Antenna-Enhanced Vibrational Signals. ACS Nano, 2012, 6, 10917-10923.	14.6	43
154	Topographically controlled growth of silver nanoparticle clusters. Physica Status Solidi - Rapid Research Letters, 2012, 6, 202-204.	2.4	0
155	Three-tiered Au nano-disk array for broadband interaction with light. Nanoscale, 2012, 4, 2847.	5.6	4
156	Surface metallic states in ultrathin Bi(001) films studied with terahertz time-domain spectroscopy. Applied Physics Letters, 2012, 100, 251605.	3.3	30
157	Surfactant Growth and Optical Studies of Plasmonic Silver Nano-Disks. E-Journal of Surface Science and Nanotechnology, 2012, 10, 239-242.	0.4	1
158	Edge States of Bi Nanoribbons on Bi Substrates: First-Principles Density Functional Study. Japanese Journal of Applied Physics, 2012, 51, 025201.	1.5	7
159	Thickness dependent phase transition of Bi films quench condensed on semiconducting surfaces. CrystEngComm, 2011, 13, 4604.	2.6	7
160	Low-energy plasmons in quantum-well and surface states of metallic thin films. Physical Review B, 2011, 84, .	3.2	10
161	Longitudinal and transverse coupling in infrared gold nanoantenna arrays: long range versus short range interaction regimes. Optics Express, 2011, 19, 15047.	3.4	94
162	Surface-enhanced ATR-IR spectroscopy with interface-grown plasmonic gold-island films near the percolation threshold. Physical Chemistry Chemical Physics, 2011, 13, 4935.	2.8	86

Ταδαακί Νάδαο

#	Article	IF	CITATIONS
163	Infrared spectroscopic and electron microscopic characterization of gold nanogap structure fabricated by focused ion beam. Nanotechnology, 2011, 22, 275202.	2.6	27
164	Low-energy Plasmons in Ultrathin Silver Structures: a Combination of Electron Energy Loss and Infrared Spectroscopy. , 2011, , .		0
165	Low-dimensional plasmons in atom-scale metallic objects. , 2010, , .		0
166	Microstructure of leached Al-Cu-Fe quasicrystal with high catalytic performance for steam reforming of methanol. Applied Catalysis A: General, 2010, 384, 241-251.	4.3	47
167	Softening versus hardening transition in surface bilayer bonding of bismuth nanofilm. Physical Review B, 2010, 82, .	3.2	7
168	One-dimensional plasmons in ultrathin metallic silicide wires of finite width. Physical Review B, 2010, 81, .	3.2	32
169	Characteristic IR Câ•€ Stretch Enhancement in Monolayers by Nonconjugated, Noncumulated Unsaturated Bonds. Langmuir, 2010, 26, 4594-4597.	3.5	5
170	Antenna Sensing of Surface Phonon Polaritons. Journal of Physical Chemistry C, 2010, 114, 7299-7301.	3.1	62
171	Plasmons in nanoscale and atomic-scale systems. Science and Technology of Advanced Materials, 2010, 11, 054506.	6.1	47
172	Optical detection of plasmonic and interband excitations in 1-nm-wide indium atomic wires. Applied Physics Letters, 2010, 96, 243101.	3.3	23
173	Relativistic Effect on the Bistability of Bi {012} Nanofilms. E-Journal of Surface Science and Nanotechnology, 2009, 7, 13-16.	0.4	0
174	Role of Oxygen Electrons in the Metal-Insulator Transition in the Magnetoresistive Oxide <mml:math xmlns:mml="http://www.w3.org/1998/Math/MathML" display="inline"><mml:msub><mml:mi>La</mml:mi><mml:mrow><mml:mn>2</mml:mn><mml:mo>â^'mathvari. Physical Review Letters, 2009, 102, 206402.</mml:mo></mml:mrow></mml:msub></mml:math 	ıo> 7.8 ml:r	nn>27
175	Studies on gold atom chains and lead nanowires on silicon vicinal surfaces. Journal of Physics: Conference Series, 2009, 187, 012025.	0.4	5
176	Thermodynamically stable nanotips of Au–Mo alloy. Journal of Vacuum Science & Technology B, 2009, 27, 2432-2434.	1.3	5
177	Optically monitored wetâ€chemical preparation of SEIRA active Au nanostructures. Surface and Interface Analysis, 2008, 40, 1681-1683.	1.8	10
178	Characterization of atomicâ€level plasmonic structures by lowâ€energy EELS. Surface and Interface Analysis, 2008, 40, 1764-1767.	1.8	5
179	Electronic Structure of Ultrathin Bismuth Films with A7 and Black-Phosphorus-like Structures. Journal of the Physical Society of Japan, 2008, 77, 014701.	1.6	73
180	Fluorine diffusion assisted by diffusing silicon on the Si(111)-(7×7) surface. Journal of Chemical Physics, 2008, 129, 234710.	3.0	6

#	Article	IF	CITATIONS
181	Growth of atomically flat nanofilms and surface superstructures of intrinsic liquid alloys. Applied Physics Letters, 2008, 92, 143116.	3.3	0
182	The excitation of one-dimensional plasmons in Si and Au–Si complex atom wires. Nanotechnology, 2008, 19, 355204.	2.6	10
183	Origin of the surface-state band-splitting in ultrathin Bi films: from a Rashba effect to a parity effect. New Journal of Physics, 2008, 10, 083038.	2.9	62
184	Disappearance of the quasi-one-dimensional plasmon at the metal-insulator phase transition of indium atomic wires. Physical Review B, 2008, 77, .	3.2	24
185	Experimental investigation of two-dimensional plasmons in a <mml:math xmlns:mml="http://www.w3.org/1998/Math/MathML" display="inline"> <mml:mrow> <mml:msub> <mml:mrow> <mml:mtext>DySi </mml:mtext> </mml:mrow> <mml:mn: on Si(111). Physical Review B. 2008. 78.</mml:mn: </mml:msub></mml:mrow></mml:math 	→2 ^{3;2} /mml:n	nn>
186	Precisely Controlled Fabrication of a Highly Sensitive Au Sensor Film for Surface Enhanced Spectroscopy. Japanese Journal of Applied Physics, 2007, 46, L1222-L1224.	1.5	8
187	Comparative Study of Atomic and Electronic Structures of P and Bi Nanofilms. Japanese Journal of Applied Physics, 2007, 46, 7824-7828.	1.5	11
188	Large surface-state conductivity in ultrathin Bi films. Applied Physics Letters, 2007, 91, .	3.3	92
189	Electronic Structures of the Highest Occupied Molecular Orbital Bands of a Pentacene Ultrathin Film. Physical Review Letters, 2007, 98, 247601.	7.8	167
190	Two-Step Desorption Process of Au Nanoparticles in D2O Suspension on Amino-Terminated SiO2/Si Substrate Induced by Small Thiol Molecules. Japanese Journal of Applied Physics, 2007, 46, 3020-3023.	1.5	6
191	Plasmon confinement in atomically thin and flat metallic films. , 2007, , .		3
192	STM/STS STUDIES OF THE INITIAL STAGE OF GROWTH OF ULTRA-THIN BI FILMS ON 7 × 7-SI(111) SURFACE. International Journal of Nanoscience, 2007, 06, 399-401.	0.7	1
193	Sound-Wave-Like Collective Electronic Excitations in Au Atom Chains. Journal of the Physical Society of Japan, 2007, 76, 114714.	1.6	23
194	Exchange-Correlation Effects on Low-Dimensional Plasmons in an Array of Metallic Quantum Wires. Materials Transactions, 2007, 48, 718-721.	1.2	12
195	In situ Surface-Enhanced Infrared Absorption Spectroscopy for the Analysis of the Adsorption and Desorption Process of Au Nanoparticles on the SiO2/Si Surface. Langmuir, 2007, 23, 6119-6125.	3.5	47
196	Direct observation of spin splitting in bismuth surface states. Physical Review B, 2007, 76, .	3.2	163
197	Quantum well states in ultrathin Bi films: Angle-resolved photoemission spectroscopy and first-principles calculations study. Physical Review B, 2007, 75, .	3.2	103
198	Origin of flat morphology and high crystallinity of ultrathin bismuth films. Surface Science, 2007, 601, 3593-3600.	1.9	79

#	Article	IF	CITATIONS
199	Adsorption and Desorption of Au Nanoparticles Monitored by Infrared Spectroscopy. IEEJ Transactions on Electronics, Information and Systems, 2007, 127, 2171-2174.	0.2	0
200	One-Dimensional Plasmon in an Atomic-Scale Metal Wire. Physical Review Letters, 2006, 97, 116802.	7.8	101
201	Stability of the quasicubic phase in the initial stage of the growth of bismuth films on Si(111)-7×7. Journal of Applied Physics, 2006, 99, 014904.	2.5	36
202	Role of Spin-Orbit Coupling and Hybridization Effects in the Electronic Structure of Ultrathin Bi Films. Physical Review Letters, 2006, 97, 146803.	7.8	289
203	Reversible adsorption of Au nanoparticles on SiO2/Si: An in situ ATR-IR study. Surface Science, 2006, 600, L71-L75.	1.9	39
204	Bias dependence of STM profiles around the quantum point contact. Surface Science, 2006, 600, 4319-4322.	1.9	0
205	Local electronic structure of a quantum point contact observed with STM. Physical Review B, 2006, 74, .	3.2	1
206	Strong lateral growth and crystallization via two-dimensional allotropic transformation of semi-metal Bi film. Surface Science, 2005, 590, 247-252.	1.9	66
207	Allotropic Transformation of Semimetal Bi Nanofilm on the Si Surface. Hyomen Kagaku, 2005, 26, 344-350.	0.0	3
208	Thin bismuth film as a template for pentacene growth. Applied Physics Letters, 2005, 86, 073109.	3.3	87
209	Hydrogen-Induced Instability of the Ge(105) Surface. Physical Review Letters, 2005, 94, 086105.	7.8	5
210	Step-by-step cooling of a two-dimensional Na gas on theSi(111)â€(7×7)surface. Physical Review B, 2004, 70, .	3.2	16
211	Bilayer-by-bilayer etching of 6H-GaN(0001) with Cl. Surface Science, 2004, 561, L213-L217.	1.9	7
212	Nanofilm Allotrope and Phase Transformation of Ultrathin Bi Film on Si(111)-7×7. Physical Review Letters, 2004, 93, 105501.	7.8	417
213	Surface pre-melting and surface flattening of Bi nanofilms on Si(111)-7×7. Surface Science, 2003, 547, L877-L881.	1.9	47
214	Tunneling conductivity features of the new reconstructed phases on the GaN(0001) surface. JETP Letters, 2003, 78, 578-582.	1.4	2
215	Na Adsorption on theSi(111)â~'(7×7)Surface: From Two-Dimensional Gas to Nanocluster Array. Physical Review Letters, 2003, 91, 126101.	7.8	110
216	Layer-by-layer growth of Ag on a GaN(0001) surface. Applied Physics Letters, 2003, 82, 1389-1391.	3.3	7

#	Article	IF	CITATIONS
217	Transformation dynamics in Ca-induced reconstructions on Si(111) surface. E-Journal of Surface Science and Nanotechnology, 2003, 1, 26-32.	0.4	2
218	STM/STS Studies of the Structural Phase Transition in the Growth of Ultra-Thin Bi Films on Si(111). Acta Physica Polonica A, 2003, 104, 381-387.	0.5	1
219	Origin of the Stability of Ge(105) on Si: A New Structure Model and Surface Strain Relaxation. Physical Review Letters, 2002, 88, 176101.	7.8	100
220	Two-dimensional plasmon in a metallic monolayer on a semiconductor surface: Exchange-correlation effects. Physical Review B, 2002, 66, .	3.2	23
221	Nonlinear mechanism of plasmon damping in electron gas. Physical Review B, 2002, 66, .	3.2	7
222	Fluorine etching on the Si()-7×7 surfaces using fluorinated fullerene. Surface Science, 2002, 521, 43-48.	1.9	12
223	Dispersion and Damping of a Two-Dimensional Plasmon in a Metallic Surface-State Band. Physical Review Letters, 2001, 86, 5747-5750.	7.8	137
224	Phase transition and stability of Si(111)–8×`2'-In surface phase at low temperatures. Surface Science, 2001, 488, 15-22.	1.9	49
225	A series of Ca-induced reconstructions on Si(111) surface. Surface Science, 2001, 493, 148-156.	1.9	58
226	Growth mode and electrical conductance of Ag atomic layers on Si(001) surface. Surface Science, 2001, 493, 389-398.	1.9	12
227	Surface roughness and electrical resistance on Si(100)2×3-Na surface. Surface Science, 2001, 493, 619-625.	1.9	8
228	Independently driven four-tip probes for conductivity measurements in ultrahigh vacuum. Surface Science, 2001, 493, 633-643.	1.9	125
229	Two-dimensional plasmon in a surface-state band. Surface Science, 2001, 493, 680-686.	1.9	19
230	Electromigration and phase transformation of Ag on a Cu-precovered Si(111) surface. Surface Science, 2001, 493, 331-337.	1.9	4
231	Electronic structure of Ag-induced3×3and21×21superstructures on the Si(111) surface studied by angle-resolved photoemission spectroscopy and scanning tunneling microscopy. Physical Review B, 2001, 64, .	3.2	49
232	Growth and electron quantization of metastable silver films on Si(001). Physical Review B, 2001, 63, .	3.2	54
233	Observation of a two-dimensional plasmon in a metallic monolayer on silicon surface. Springer Proceedings in Physics, 2001, , 875-876.	0.2	0
234	Construction of an ELS-LEED: an electron energy-loss spectrometer with electrostatic two-dimensional angular scanning. Surface and Interface Analysis, 2000, 30, 488-492.	1.8	11

#	Article	IF	CITATIONS
235	Surface electronic transport on silicon: donor- and acceptor-type adsorbates on Si(111)-â^š3×â^š3-Ag substrate. Applied Surface Science, 2000, 162-163, 42-47.	6.1	16
236	Diffusion anisotropy of Ag and In on Si(111) surface studied by UHV-SEM. Ultramicroscopy, 2000, 85, 23-33.	1.9	7
237	MICRO-FOUR-POINT PROBES IN A UHV SCANNING ELECTRON MICROSCOPE FOR IN-SITU SURFACE-CONDUCTIVITY MEASUREMENTS. Surface Review and Letters, 2000, 07, 533-537.	1.1	34
238	Epitaxial Growth of Single-Crystal Ultrathin Films of Bismuth on Si(111). Japanese Journal of Applied Physics, 2000, 39, 4567-4570.	1.5	46
239	Substrate-Structure Dependence of Ag Electromigration on Au-Precovered Si(111) Surfaces. Japanese Journal of Applied Physics, 2000, 39, 4438-4442.	1.5	4
240	Surface-State Bands on Silicon –Si(111)-\$sqrt{3}imessqrt{3}\$-Ag Surface Superstructure–. Japanese Journal of Applied Physics, 2000, 39, 3815-3822.	1.5	55
241	Construction of an ELS–LEED: an electron energy-loss spectrometer with electrostatic two-dimensional angular scanning. , 2000, 30, 488.		1
242	Instability and Charge Density Wave of Metallic Quantum Chains on a Silicon Surface. Physical Review Letters, 1999, 82, 4898-4901.	7.8	543
243	Structure ofC60layers on theSi(111)â^'3×3â^'Agsurface. Physical Review B, 1999, 60, 11131-11136.	3.2	39
244	Two-dimensional adatom gas phase on the Si(111)-3×3-Ag surface directly observed by scanning tunneling microscopy. Physical Review B, 1999, 60, 16083-16087.	3.2	49
245	Structural phase transitions of Pb-adsorbed Si(111) surfaces at low temperatures. Physical Review B, 1999, 60, 13287-13290.	3.2	76
246	Structures and electronic transport on silicon surfaces. Progress in Surface Science, 1999, 60, 89-257.	8.3	210
247	Electron standing waves on the Si(111)-3×3-Ag surface. Physical Review B, 1999, 59, 2035-2039.	3.2	57
248	Morphology of ultrathin manganese silicide on Si(111). Surface Science, 1999, 419, 134-143.	1.9	51
249	Si(111)-(×)-Ag surface at low temperatures: symmetry breaking and surface twin boundaries. Surface Science, 1999, 442, 65-73.	1.9	114
250	Diffraction from small antiphase domains: α-, β-, 6×6 phases of Au adsorbed Si(111). Applied Surface Science, 1998, 130-132, 47-53.	6.1	11
251	STM observations of Ag adsorption on the Si(111)– surface at low temperatures. Surface Science, 1998, 408, 146-159.	1.9	48
252	Deformation of boron networks at the LaB6(111) surface. Surface Science, 1998, 416, 363-370.	1.9	12

#	Article	IF	CITATIONS
253	Surface Electrical Conduction Correlated with Surface Structures and Atom Dynamics. Surface Review and Letters, 1998, 05, 803-819.	1.1	12
254	Structural phase transitions ofSi(111)â^'(3×3)R30°â^'Au: Phase transitions in domain-wall configurations. Physical Review B, 1998, 57, 10100-10109.	3.2	106
255	Structures and Electrical Conduction on Silicon Surfaces. Hyomen Kagaku, 1998, 19, 114-121.	0.0	1
256	Structures and Electrical Conduction on Silicon Surfaces Hyomen Kagaku, 1998, 19, 193-200.	0.0	0
257	Surface phonons of Na-induced superstructures on Al(111). Physical Review B, 1997, 55, 10064-10073.	3.2	18
258	Surface electrical conduction due to carrier doping into a surface-state band on Si(111)-3×3-Ag. Physical Review B, 1997, 56, 6782-6787.	3.2	94
259	Critical scattering at the order-disorder phase transition of Si(111)-3×3R30°-Au surface: A phase transition with particle exchange. Physical Review B, 1997, 55, 8129-8135.	3.2	23
260	Electrical conduction via surface-state bands. Surface Science, 1997, 386, 322-327.	1.9	44
261	Surface Phonons of Lanthanum Hexaboride and its Thermionic Properties Shinku/Journal of the Vacuum Society of Japan, 1997, 40, 77-83.	0.2	0
262	Oxygen adsorption sites on the PrB6(100) and LaB6(100) surfaces. Surface Science, 1996, 348, 133-142.	1.9	33
263	Oxygen adsorption on LaB6 (100) and (111) surfaces. Surface Science, 1996, 357-358, 708-711.	1.9	17
264	Surface phonon dispersion curves of the LaB6(111) surface. Surface Science, 1996, 357-358, 712-716.	1.9	8
265	Two-dimensional adatom gas on the Si(111)-(â^š3×â^š3)-Ag surface detected through changes in electrical conduction. Physical Review B, 1996, 54, 14134-14138.	3.2	35
266	Vibrational spectra of oxygen on LaB6(100), (110), and (111) surfaces: A comparative study using high resolution electron energy loss spectroscopy. Journal of Vacuum Science and Technology A: Vacuum, Surfaces and Films, 1996, 14, 1674-1678.	2.1	8
267	Vibrations of alkali-metal atoms chemisorbed on the Al(111) surface. Surface Science, 1995, 329, 269-275.	1.9	23
268	Construction of a highâ€resolution electron energy loss spectrometer. Review of Scientific Instruments, 1994, 65, 515-516.	1.3	16
269	Surface atomic structure and surface force constants: Cu(100)2â^š2 × â^š2-R45°-O and LaB6(100). Surface Science, 1993, 298, 450-455.	1.9	4
270	Deformation of octahedra at LaB6(100) surface studied by HREELS. Surface Science, 1993, 287-288, 391-395.	1.9	17

#	Article	IF	CITATIONS
271	Surface Phonon Dispersion Curves of NiAl(111). Japanese Journal of Applied Physics, 1993, 32, 3252-3256.	1.5	8
272	Fano resonance of optical phonons in a multilayer graphene stack. Japanese Journal of Applied Physics, 0, , .	1.5	0
273	Optical Properties and Optimization of LaB ₆ Thin Films for Photothermal Applications. Advanced Optical Materials, 0, , 2101787.	7.3	3